ACKNOWLEDGMENT

The authors wish to thank M. Ashiki for his help in the construction of the system and measurements and Dr. S. Mizushina for valuable discussions and suggestions on the manuscript.

REFERENCES

[1] J. R. Ashley, C. B. Searles, and F. M. Palka, "The measurement of oscillator noise at microwave frequencies," *IEEE Trans. Microwave Theory Tech.*, vol. MTT-16, pp. 753–760, Sept. 1968.
[2] J. G. Ondria, "A microwave system for measurements of AM and FM noise spectra," *IEEE Trans. Microwave Theory Tech.*, vol. MTT-16, pp. 767–781, Sept. 1968.
[3] J. L. Fikart, J. Nigrin, and P. A. Goud, "The accuracy of AM and FM noise measurements employing a carrier suppression filter and phase detector," *IEEE Trans. Microwave Theory Tech.* (Short Papers), vol. MTT-20, pp. 702–703, Oct. 1972.
[4] J. L. Fikart and P. A. Goud, "The direct-detection noise-measuring system and its threshold," *IEEE Trans. Instrum. Meas.*, vol. IM-21, pp. 219–224, Aug. 1972.

A Numerical Method Based on the Discretization of Maxwell Equations in Integral Form

M. ALBANI AND P. BERNARDI, SENIOR MEMBER, IEEE

***Abstract*—A method is described for the solution of the electromagnetic field inside resonant cavities and waveguides of arbitrary shape, whether homogeneously or inhomogeneously filled. The method, suitably programmed for use with a digital computer, is based on the direct discretization of the Maxwell equations in integral form. Since the method works with the components of the electromagnetic field, the numerical solution directly gives the distributions of the field in the structure, in addition to the resonant frequencies of cavities or the propagation constants of waveguides. Some numerical applications of the method are given.**

I. INTRODUCTION

Numerous satisfactory numerical methods are available today for determining the electromagnetic field, both in structures in which the field can be derived from a single scalar potential, as in the case of empty guides of arbitrary shape [1]–[3], and in more general structures in which the field has all the components differing from 0, such as waveguides loaded with axial dielectrics [4]–[9] or resonant cavities of arbitrary shape, whether empty or loaded with dielectric regions [8]. Comparative discussions of these methods [2], [3], [7] show that "no single solution method has proved to be best for all requirements that might be imposed."

In this short paper, a method based on the direct discretization of the Maxwell equations in integral form is presented. The method does not require the introduction of auxiliary potential functions or the use of particular analytical procedures to formulate the problem in a computationally convenient form, and it therefore represents a very direct approach for the solution of a large class of structures. Moreover, the method presented allows the solution, with unified treatment, of both two- and three-dimensional structures.

II. DISCRETIZATION OF MAXWELL'S EQUATIONS IN INTEGRAL FORM

Considering a source-free region and assuming $\exp[j\omega t]$ as time dependence, Maxwell's equations in integral form may be written

$$\oint_s \boldsymbol{t}\cdot\boldsymbol{E}\,ds = -\int_S \boldsymbol{n}\cdot\boldsymbol{H}\,dS \tag{1a}$$

$$\oint_s \boldsymbol{t}\cdot\boldsymbol{H}\,ds = -\int_S \epsilon_r(P)\boldsymbol{n}\cdot\boldsymbol{E}\,dS \tag{1b}$$

where $\epsilon_r(P)$ is the permittivity of the medium in the structure. In (1) the lengths and the electric field are normalized to $1/\omega(\mu_0\epsilon_0)^{1/2}$ and $j(\mu_0/\epsilon_0)^{1/2}$, respectively; that is,

$$s = \omega(\mu_0\epsilon_0)^{1/2}\bar{s} \tag{2a}$$

$$\boldsymbol{E} = -j\bar{\boldsymbol{E}}/(\mu_0/\epsilon_0)^{1/2} \tag{2b}$$

where $\bar{s}$ and $\bar{\boldsymbol{E}}$ are the effective length and electric field.

A. Cavities of Arbitrary Shape Inhomogeneously Filled

A cavity of arbitrary shape, bounded by a perfect conductor, and loaded with an inhomogeneous dielectric medium is considered first. In order to obtain a finite set of algebraic equations, a finite-difference procedure of discretization, the cell method [10], [11], is followed. The method consists of subdividing the cavity into cubic cells of side h, each assumed homogeneously filled, and considering the field as a function defined on the cells. Two types of cell may be considered: internal and boundary cells (Fig. 1). For all the cells of the structure, we assume the following hypotheses on the distribution of the electromagnetic field. 1) Inside each cell the components of the field have constant value. 2) On the interface between two contiguous cells, the components of the field have a value equal to the mean of the values in the two cells considered.

In this way, the continuous electromagnetic field is replaced by a set of discrete values. By applying (1a) and (1b) to each cell of the structure, we obtain a finite system of simultaneous algebraic equations. Assuming a rectangular coordinates set (x, y, z), for the generic internal cell we have

$$2hH_x + E_y(z-h) - E_y(z+h) + E_z(y+h) - E_z(y-h) = 0 \tag{3a}$$

$$2hE_x + \epsilon_r^{-1}[H_y(z-h) - H_y(z+h) + H_z(y+h) - H_z(y-h)] = 0 \tag{3b}$$

where H_x stands for $H_x(x,y,z)$ and $E_y(z-h)$ stands for $E_y(x,y,z-h)$.

The other four equations are obtained with two successive permutations of the coordinate index in (3a) and (3b). For each internal cell, six equations analogous to the preceding ones may be written; the only point to be noted is that the value of ϵ_r must be that of the medium filling the cell. At the boundary cells the electric field is assumed to be 0, while the magnetic field is assumed to be different from 0 because of the surface currents J_s on the boundary, which have not been taken into account in (1). With these hypotheses, from (1a) we obtain for the boundary cell Q of Fig. 1:

$$2hH_{xQ} = 0 \tag{4a}$$

$$2hH_{yQ} - E_{zP} = 0 \tag{4b}$$

$$2hH_{zQ} - E_{yP} = 0. \tag{4c}$$

Applying (3) and (4) to all the cells of the structure, we obtain a homogeneous system of equations that can be expressed as a matrix eigenvalue problem:

$$(A - 2hI)x = 0 \tag{5}$$

where A has not more than four nonzero elements for each row.

Because of the high number of equations necessary to obtain the field distribution with a fair degree of approximation, the eigenvalue problem can be solved numerically only with iterative methods [1].

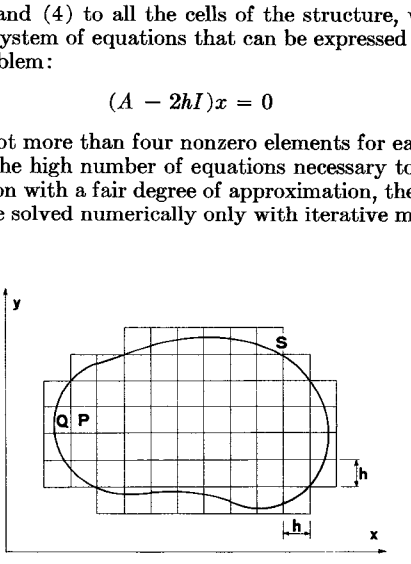

Fig. 1. Cross section of a cavity of arbitrary shape. S is the cavity boundary, P an internal cell, Q a boundary cell.

Manuscript received January 31, 1973; revised October 3, 1973. This work was supported by the Consiglio Nazionale delle Ricerche, Italy.
M. Albani is with Texas Instruments Semiconductors, Rome, Italy.
P. Bernardi is with the Istituto di Elettronica, Universita di Roma, Rome, Italy.

However, the solution of (5) by iterative methods is not easy in view of the particular structure of the matrix A [10]. In fact, this matrix has all zeros on the main diagonal and, moreover, it has pairs of equal and opposite eigenvalues. It is therefore advisable to reformulate the problem in such a way as to obtain an eigenvalue problem again, but relative to a new matrix having a structure more suitable for the use of iterative methods. The procedure consists in eliminating from (5) the components of the magnetic field, obtaining a system of equations having as unknowns only the components of the electric field in the internal cells of the structure. In particular, for each cell we obtain

$$\begin{aligned}(4h^2 - 4\epsilon_r^{-1})E_x + \epsilon_r^{-1}[&E_x(z-2h) - E_z(x-h,z-h)\\ &+ E_z(x+h,z-h) + E_x(z+2h) + E_z(x-h,z+h)\\ &- E_z(x+h,z+h) - E_y(x+h,y+h) + E_y(x-h,y+h)\\ &+ E_x(y+2h) + E_y(x+h,y-h) - E_y(x-h,y-h)\\ &+ E_x(y-2h) = 0 \end{aligned} \tag{6}$$

the remaining two equations being obtained with two successive permutations of the coordinate index.

Applying (6) to all internal cells, with due regard to the condition $\boldsymbol{E} = 0$ on the boundary cells, a matrix eigenvalue problem is obtained:

$$(B - 4h^2 I)x = 0. \tag{7}$$

Matrix B is less sparse than A, since up to 13 elements may be different from 0 in each row, but the dimensions of B are less than half those of A. Moreover, it is to be noted that all the elements of the main diagonal of B are different from 0. Another advantage of (7), compared with (5), is found in the cases in which the eigenvalues of A are all real as, for example, in the case of a cavity homogeneously filled with a lossless dielectric. In such a case, B is positive semidefinite, and it is therefore particularly easy to solve the eigenvalue problem by iterative methods. In conclusion, (7) is adopted as a basis for the solution of inhomogeneously filled cavities of arbitrary shape: the eigenvalues give, through (2a), the resonant frequencies and the eigenvectors give the relative distributions of the electric field.

The simplicity of the method discussed lies in the fact that (6) is directly applicable by assigning the appropriate permittivity to each cell, without taking account of the conditions of continuity of the tangential components at the interface between different media. Also, for the boundary conditions no problem arises, since in all the boundary cells we can put directly $\boldsymbol{E} = 0$, and (6) is not applied.

B. Dielectric Loaded Cylindrical Waveguides

We consider a waveguide section of length h, subdivided into cubic cells, each homogeneously filled. A space dependence $\exp(-k_z z)$, where z is the longitudinal axis of the guide, is assumed.

In the transverse xy plane, the same hypotheses on the distribution of the electromagnetic field as in Section I are advanced. Following the procedure described in Section I and taking account of the exponential dependence on z, for the generic internal cell we derive six equations for the components of the field. As in the case of the cavities, it is good to eliminate the magnetic field components, obtaining three equations in the electric field components:

$$\begin{aligned}[4h^2 + \epsilon_r^{-1}(4k_z^2h^2 - 2)]E_x + 2\epsilon_r^{-1}k_z h[&E_z(x+h) - E_z(x-h)]\\ &+ \epsilon_r^{-1}[E_x(y+2h) + E_x(y-2h) - E_y(x+h,y+h)\\ &+ E_y(x-h,y+h) + E_y(x+h,y-h) - E_y(x-h,y-h)]\\ &= 0 \end{aligned} \tag{8a}$$

$$\begin{aligned}[4h^2 + \epsilon_r^{-1}(4k_z^2h^2 - 2)]E_y + 2\epsilon_r^{-1}k_z h[&E_z(y+h) - E_z(y-h)]\\ &+ \epsilon_r^{-1}[E_y(x-2h) + E_y(x+2h) - E_x(x-h,y-h)\\ &+ E_x(x-h,y+h) + E_x(x+h,y-h) - E_x(x+h,y+h)]\\ &= 0 \end{aligned} \tag{8b}$$

$$\begin{aligned}(4h^2 - 4\epsilon_r^{-1})E_z + 2\epsilon_r^{-1}k_z h[&E_x(x+h) - E_x(x-h)\\ &+ E_y(y+h) - E_y(y-h)] + \epsilon_r^{-1}[E_z(y-2h)\\ &+ E_z(y+2h) + E_z(x+2h) + E_z(x-2h)] = 0. \end{aligned} \tag{8c}$$

Equations (8a)–(8c) are evaluated at each internal cell, with the condition $\boldsymbol{E} = 0$ at the boundary cells. A set of simultaneous equations is obtained that may be reduced to an eigenvalue problem by putting

$$k_z h = \text{constant}. \tag{9}$$

With this position, the matrix eigenvalue problem may be written

$$(C - 4h^2 I)x = 0 \tag{10}$$

where the elements of the matrix C are independent of h.

The eigenvalues of C give the frequencies of the waveguide modes corresponding to the value of the propagation constant given by (9); the relative distributions of $\boldsymbol{E}$ are given directly by the eigenvectors. In this way it is also possible to obtain the dispersion curves of the various modes by solving (10) for various values of $k_z h$. In particular, by putting $k_z h = 0$, the cutoff eigenvalues h_c can be obtained, as well as the relative field distributions. It may be noted that with the proposed method, the eigenvalue problem (10) is relative to a matrix C that, for homogeneously loaded guides, is always symmetric, for both TE and TM modes. As is known, this does not occur for TE modes when using the finite-difference method, unless a variational formulation is followed. Moreover, the method proposed gives, for any structure, a matrix eigenvalue problem in standard form, while, for instance, the conventional finite-element method [6] leads to a matrix eigenvalue problem in general form.

It is interesting to derive directly from (8) some well-known properties of waveguides as, for instance: in a uniform waveguide the transverse distribution of the field is independent of the propagation constant. Let us refer, for example, to TM modes. Putting $k_z = 0$, the eigenvalue problem is expressed by

$$(D - 4h_c^2 I)x = 0. \tag{11}$$

For $k_z \neq 0$, on the other hand, we have

$$[D - 4h^2(1 + \epsilon_r^{-1}k_z^2)I]x = 0. \tag{12}$$

Since in (11) and (12) the matrix D is the same, the eigenvectors (and hence the field distributions) do not vary with k_z. Moreover, from (11) and (12)

$$h_c^2 = h^2(1 + \epsilon_r^{-1}k_z^2) \tag{13}$$

which represents the well-known dispersion equation for uniform waveguides. On the contrary, for inhomogeneously loaded waveguides, from (10) we obtain a group of eigenvectors that is different for each value of k_z. This means that the distribution of the field for a given mode does not depend only on the geometry of the structure but also on the value of k_z.

III. COMPUTED RESULTS

A. General Remarks

Two general programs have been written to analyze dielectric loaded waveguides and cavities by the proposed method. The programs require as input the number and the coordinates of the cells and the value of the permittivity on each cell for the case of cavities, while for the case of waveguides it is necessary to give also the desired value of the propagation constant. In the numerical computation, account has been taken of the fact that the resulting set of equations consists of independent groups of equations. This means that in order to determine the electromagnetic field in a given structure, it is sufficient to solve an eigenvalue problem for a matrix considerably smaller than the initial one. For example, in [12] it is shown that for a resonator subdivided into 75 internal cells it is sufficient to solve an eigenvalue problem of order 20 instead of the initial one of order 225.

B. Results

1) *Uniform Waveguides*: For TM waves the eigenvalue problem obtained by (8) with $k_z = 0$ is identical to that obtained by applying the finite-difference method to the Helmholtz equation for the scalar potential $\phi = E_z$ [13], provided that the mesh length is $2h$. The results obtained are therefore equal to those in [13] and [14]. It is more interesting to examine the solutions relative to TE waves. In

fact, (8) operates on the transverse E-field components instead of on the longitudinal H_z component, as in the finite-difference method. Of course, the relative boundary conditions are also posed in a different manner. Table I shows the results obtained for an empty rectangular guide for the dominant mode, for a TE higher order mode and for a TE_{11} mode. It may be noted that the error varies with h in the same way as in the finite-difference method [13].

2) *Inhomogeneously Loaded Waveguides*: In this case, the eigenvalues can be obtained by (8) with assigned values of $k_z a$ ($k_z = \alpha_{z+j}\beta_z$). As examples, the structures of Figs. 2–4 have been solved. For the structure of Fig. 2, the results for the dominant mode are shown in Table II. The associated electric field distributions are also shown in Fig. 2. It may be noted that in this case, as h/a decreases, the error decreases about linearly with h. This result may be used, as already done for empty guides [13], for computing extrapolated eigenvalues. For the structure of Fig. 3, in which there are material discontinuities in two dimensions, the results are given in Table III and are compared with those obtained by Schlosser and Unger [15]. The structure of Fig. 4, consisting of a square waveguide loaded with a dielectric rod, has been chosen as an example of the application of the method to a structure in which the material boundary does not consist of parts of straight lines; the results are compared, in Table IV, with those obtained by Bates and Ng [9]. It may be noted that with a mesh of 20 × 20 cells, corresponding to 261 equations, the results are almost coincident with those given in [9].

In the above examples the numerical computation has been carried out starting from the general equations (8a)–(8c) without

TABLE I
EMPTY RECTANGULAR WAVEGUIDE: TE MODES

Mode	h/a	Computed $k_o a$	Error, %	Error Dependence
TE_{10}	1/18	3.1257	0.51	$\simeq h^2$
	1/36	3.1376	0.13	
true $k_o a$ = 3.1416	1/72	3.1406	0.03	
TE_{30}	1/18	9.0000	4.51	$\simeq h^2$
	1/36	9.3175	1.14	
true $k_o a$ = 9.4248	1/72	9.3979	0.29	
TE_{11} (b/a = 2/3)	1/6	5.1962	8.25	$\simeq h^2$
	1/12	5.5439	2.11	
true $k_o a$ = 5.6637	1/24	5.6334	0.53	

TABLE II
WAVEGUIDE IN FIG. 2: DOMINANT TE MODE

$\beta_z a$	h/a	True $k_o a = \omega\sqrt{\mu\epsilon_r}\,a$	Computed $k_o a$	Error, %	Error Dependence	Computer Time
0	1/12	1.0674	1.1828	10.81	$\simeq h$	
	1/36		1.0239	- 4.08		< 20s
	1/108		1.0817	1.34		
	1/324		1.0630	- 0.41		< 60s
2	1/12	1.2513	1.3744	9.84	$\simeq h$	
	1/36		1.2017	- 3.96		< 20s
	1/108		1.2674	1.29		
	1/324		1.2470	- 0.34		< 60s
4	1/12	1.6613	1.7807	7.19	$\simeq h$	
	1/36		1.5991	- 3.74		< 20s
	1/108		1.6810	1.19		
	1/324		1.6560	- 0.32		< 60s

TABLE III
WAVEGUIDE IN FIG. 3: DOMINANT MODE

$\beta_z a$	h/a	Computed $k_o a$	Schlosser and Unger $k_o a$	Error, %	Computer Time
1	1/10	1.98	2.12	6.6	<20s
	1/20	2.05		3.3	<60s
2	1/10	2.11	2.25	6.2	<20s
	1/20	2.18		3.1	<60s

TABLE IV
WAVEGUIDE IN FIG. 4: DOMINANT TE MODE AT CUTOFF

d/a	Computed $k_c a$	Bates and Ng $k_o a$ Measured	Bates and Ng $k_o a$ Computed	Computer Time
0.0	2.936	2.865	2.958	< 60s
0.206	2.982	2.904	2.982	< 60s

Note: $h/a = 1/20$.

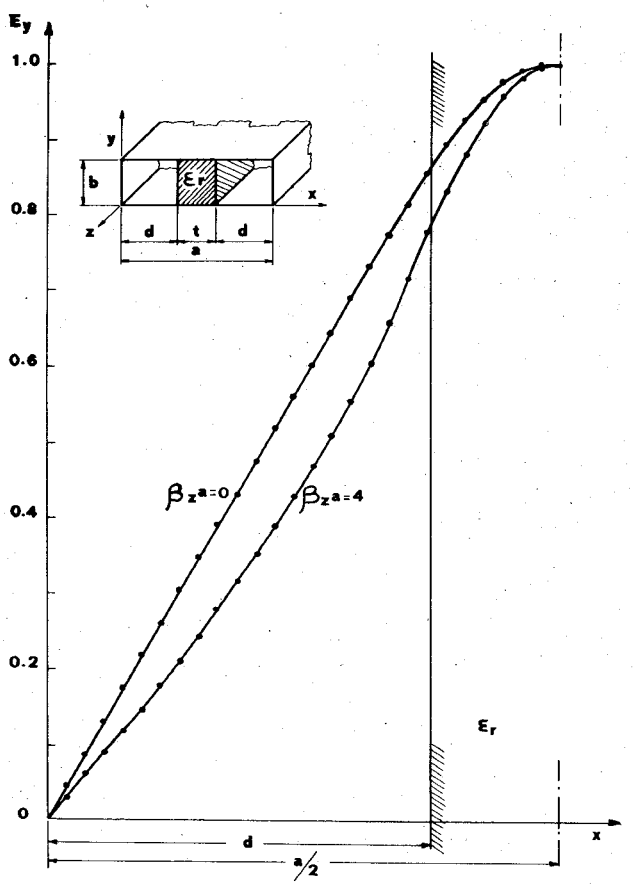

Fig. 2. E-field distribution for the dominant mode in the considered guide. Lines denote theoretical curves, dots denote computed values. $\epsilon_r = 16$, $t/a = 1/4$, $b/a = 4/9$.

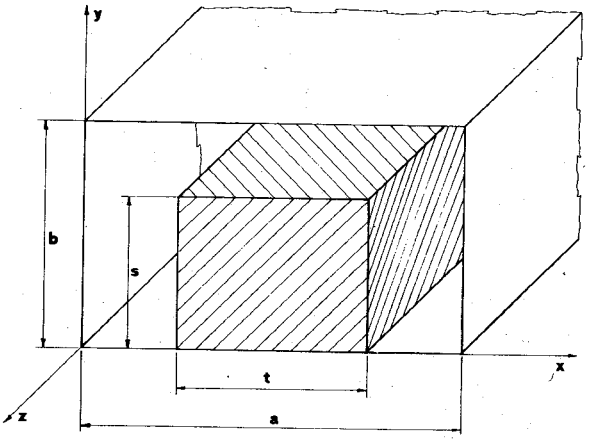

Fig. 3. Rectangular waveguide with insert at center of bottom wall. $\epsilon_r = 6$, $t/a = 1/2$, $b/a = 3/5$, $s/a = 2/5$.

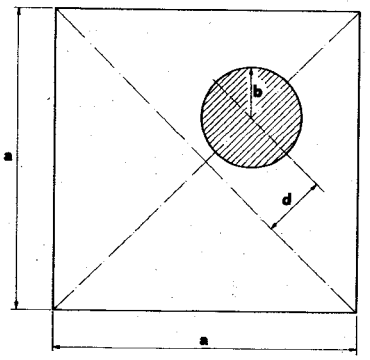

Fig. 4. Square waveguide loaded with dielectric rod. $\epsilon_r = 2.30$, $b/a = 0.161$.

taking any advantage of the particular symmetries. For example, in the case of Table IV, since the computation is carried out at cutoff, we could have obtained the TE modes by putting $E_z = 0$ directly in (8), thus considerably reducing the computer time. Therefore, with the same time shown in Table IV, we can calculate points of the dispersion curves for hybrid modes at any frequency. In Table II, where account has been taken of the existence of TE zero-order modes, the computer time is much shorter.

Finally, we considered the structure studied by Franceschetti [16] consisting of a rectangular guide completely filled with an inhomogeneous dielectric whose permittivity is $\epsilon_r(x) = 5 \exp(-1.61x/a)$ (a is the larger dimension of the guide). The results are shown in Table V and Fig. 5.

3) *Homogeneous Cavities*: By applying (6) to the case of a rectangular cavity, the results shown in Table VI are obtained. As may be seen, even with a moderate number of equations the resonant frequencies of the first modes are obtained with errors smaller than 1 percent.

4) *Inhomogeneously Loaded Cavities*: As numerical examples we considered: a) the cavities obtained from the waveguides in Figs. 2 and 3; and b) the cavity of Fig. 6.

The structures in Figs. 2 and 3, because of their cylindrical symmetry, may be solved either by applying (8) of the waveguides after assuming $\beta_z h = m\pi h/c$ ($m = 1, 2, \cdots$), or by directly applying (6) of the cavities. For these structures both methods have been applied. For cavities of arbitrary shape, on the other hand, like that shown in Fig. 6, only (6) can be applied, in view of the absence of any symmetry.

The results given in Table VII show the following. 1) For cavities with cylindrical symmetry, it is advisable to use (8) instead of (6). 2) The errors obtained via (6) are of the same order of magnitude for structures inhomogeneous in one direction only (Fig. 2), in two directions (Fig. 3), and in all three directions (Fig. 6).

TABLE V
RECTANGULAR GUIDE COMPLETELY FILLED WITH INHOMOGENEOUS DIELECTRIC: DOMINANT TE MODE

$\beta_z a$	h/a	Computed $k_0 a$	Franceschetti $k_0 a$	Computer Time
10.209	1/40	6.276	6.283	< 20s
	1/60	6.280		
	1/100	6.282		

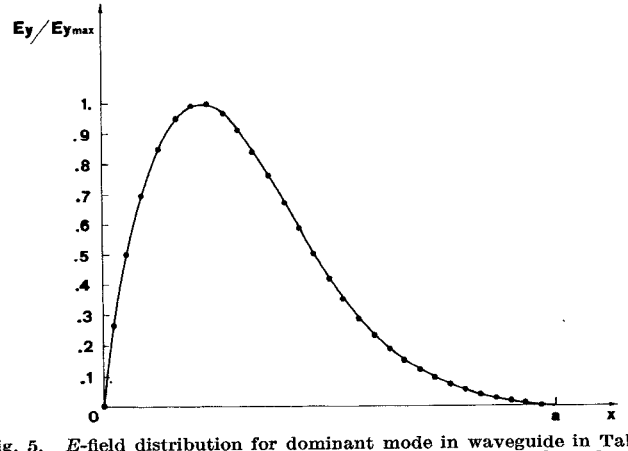

Fig. 5. E-field distribution for dominant mode in waveguide in Table V ($\beta_z a = 10.209$). Line denotes Franceschetti curve, dots denote computed values.

TABLE VI
EMPTY RECTANGULAR RESONATOR (a,b,c)

Mode	h/a	Computed $k_0 a$	Error, %	Number of Equations
TM_{110} True resonant freq. $k_0 a = 5.6636$	1/12	5.5439	2.11	121
	1/24	5.6335	0.53	1322
TE_{101} True $k_0 a = 7.0249$	1/12	6.7560	3.83	121
	1/24	6.9571	0.97	1322
TM_{210}, TE_{011} True $k_0 a = 7.8540$	1/12	7.5558	3.80	121
	1/24	7.7784	0.96	1322

Note: $b/a = 2/3$, $c/a = 1/2$.

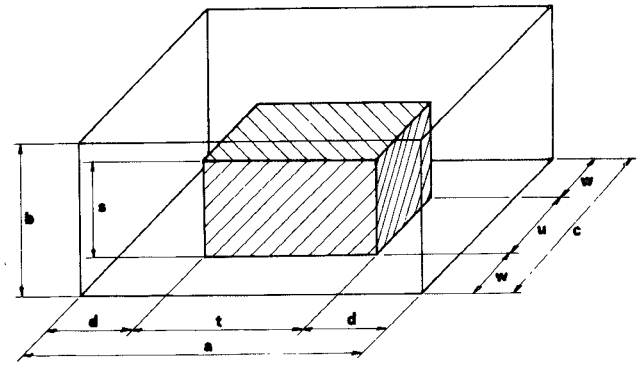

Fig. 6. Rectangular cavity with dielectric insert. $\epsilon_r = 2.05$, $b/a = 4/9$, $c/a = 5/9$, $u/a = 2/9$, $s/a = 5/18$, $t/a = 1/2$.

TABLE VII
INHOMOGENEOUSLY LOADED RESONATORS: DOMINANT MODE

Resonator	Resonant Frequency $k_0 a$		Error, %	Computer Time
Fig. 2	True $k_0 a$ (TE_{101} mode)	2.583	-	
Resonator length c/a=4/10	$k_0 a$ computed via (8)	2.429	6.0	< 10s
h/a = 1/20	$k_0 a$ computed via (6)	2.383	7.7	< 60s
Fig. 3	Schlosser& Unger $k_0 a$	2.73	-	
Resonator length c/a=4/5	$k_0 a$ computed via (8)	2.59	5.1	< 10s
h/a = 1/10	$k_0 a$ computed via (6)	2.56	6.2	< 60s
Fig. 6	Measured $k_0 a$	5.22	-	
h/a = 1/18	Computed $k_0 a$	5.55	6.3	< 60s

IV. CONCLUSIONS

The method presented may be applied to a wide class of structures, such as cylindrical waveguides and cavities of arbitrary shape, even if inhomogeneously filled. Although the electromagnetic field has been approximated with constant values in the cells, the method gives, with good approximation, both the field distributions and the resonant frequencies or the propagation constants with a moderate number of equations. The complexity of the numerical solution and the computing time depend only on the number of cells into which the structure is subdivided and are not influenced by the presence of one or more dielectrics inside it.

REFERENCES

[1] A. Wexler, "Computation of electromagnetic fields," *IEEE Trans. Microwave Theory Tech. (Special Issue on Computer-Oriented Microwave Practices)*, vol. MTT-17, pp. 416–439, Aug. 1969.

[2] J. B. Davies, "Numerical solution of the hollow waveguide problem," in *Progress in Radio Science*, vol. 3. Brussels, Belgium: International Scientific Radio Union, 1971, pp. 307–320.

[3] B. E. Spielman and R. F. Harrington, "Waveguides of arbitrary cross section by solution of nonlinear integral eigenvalue equation," *IEEE Trans. Microwave Theory Tech.*, vol. MTT-20, pp. 578–585, Sept. 1972.

[4] W. J. English, "Vector variational solutions of inhomogeneously loaded cylindrical waveguide structures," *IEEE Trans. Microwave Theory Tech.*, vol. MTT-19, pp. 9–18, Jan. 1971.

[5] W. J. English and F. J. Young, "An E vector variational formulation of the Maxwell equations for cylindrical waveguide problems," *IEEE Trans. Microwave Theory Tech.*, vol. MTT-19, pp. 40–46, Jan. 1971.

[6] Z. J. Csendes and P. Silvester, "Numerical solution of dielectric loaded waveguides: I—Finite-element analysis," *IEEE Trans. Microwave Theory Tech. (1970 Symposium Issue)*, vol. MTT-18, pp. 1124–1131, Dec. 1970.

[7] ——, "Numerical solution of dielectric loaded waveguides: II—Modal approximation technique," *IEEE Trans. Microwave Theory Tech.*, vol. MTT-19, pp. 504–509, June 1971.

[8] R. F. Harrington, in *Field Computation by Moment Methods*. New York: Macmillan, 1968.

[9] R. H. T. Bates and F. L. Ng, "Polarisation-source formulation of electromagnetism and dielectric-loaded waveguides," *Proc. Inst. Elec. Eng.*, vol. 119, pp. 1568–1574, Nov. 1972.

[10] G. E. Forsythe and W. R. Wasow, *Finite-Difference Methods for Partial Differential Equations*. New York: Wiley, 1960.

[11] G. Liebmann, "Resistance-network analogues with unequal meshes or subdivided meshes," *Brit. J. Appl. Phys.*, vol. 5, pp. 362–366, Oct. 1954.

[12] M. Albani and P. Bernardi, "A numerical method for six-component electromagnetic fields," Inst. Elettronica, Univ. Roma, Rome, Italy, Internal Rep. 51, Feb. 1973.

[13] J. B. Davies and C. A. Muilwyk, "Numerical solution of uniform hollow waveguides with boundaries of arbitrary shape," *Proc. Inst. Elec. Eng.*, vol. 113, pp. 277–284, Feb. 1966.

[14] M. J. Beaubien and A. Wexler, "An accurate finite-difference method for higher order waveguide modes," *IEEE Trans. Microwave Theory Tech. (1968 Symposium Issue)*, vol. MTT-16, pp. 1007–1017, Dec. 1968.
[15] W. Schlosser and H. G. Unger, "Partially filled waveguides of rectangular cross section," in *Advances in Microwaves*, vol. 1. New York: Academic, 1966.
[16] G. Franceschetti, "Eigenvalues and eigenfunctions of transversely inhomogeneous rectangular waveguides," *Alta Freq.*, vol. 32, pp. 133–141, Feb. 1963.

Low-Noise Mixer in Oversized Microstrip for 5-mm Band

PAUL J. MEIER

Abstract—**This short paper summarizes the design and performance of a low-noise 5-mm mixer constructed in oversized microstrip—a new type of transmission line which is superior to microstrip at millimeter wavelengths. Including a 5-dB IF contribution, the measured noise figure was 9–10.5 dB over a wide range of LO frequencies and drive levels.**

Although standard microstrip techniques can be applied to millimeter components [1]–[3], several problems arise. These problems include critical tolerances, fragile substrates, thin conductor strips which are not completely compatible with hybrid devices, and difficulty in obtaining a simple transition to conventional waveguide. Mounting an integrated circuit between two waveguides [4], can alleviate these problems. This short paper discusses the design and performance of a low-noise wide-band millimeter mixer constructed in a new IC medium called oversized microstrip [5].

Normally, the thickness of a microstrip substrate is held to a small fraction of a guided quarter wavelength to restrict the radiation loss. If, however, we intentionally set the substrate thickness at a quarter wavelength, an efficient radiator may be printed on the ungrounded surface of the substrate. When mounted in a waveguide, as shown in Fig. 1, this radiator will couple to the TE_{10} waveguide mode and all the power may be delivered to an impedance-matched load (such as a mixer diode) provided that no energy is reradiated in some other mode such as the crossed TE_{01} mode. For this reason, the air-filled portion of the waveguide should not support the TE_{01} mode, which is automatically accomplished when a standard waveguide is operated within its normal frequency range. Moreover, the dielectric-filled portion of the waveguide should not support the TE_{01} mode, in order to prevent resonances within the substrate. This may be accomplished by reducing the waveguide size within the dielectric region, or by printing the radiator on a thin substrate which is suspended above the ground plane.

Fig. 1 illustrates the essential features of a mixer constructed in oversized microstrip. Both the local oscillator and the signal are coupled from the waveguide by a monopole, whose length and shape are selected to provide a wide-band impedance match to the diode. In the intended application, both the local oscillator and signal will be close in frequency, and fed to an array of mixers by quasi-optical techniques. (A small local-oscillator radiator illuminates the mixer array which is located in the focal region of a large spherical reflector.) Laboratory testing of each mixer is performed, external to the array, by injecting the local oscillator through a directional coupler. In each mixer, the diode is returned to ground at RF and dc by a direct connection to the waveguide housing. Bias is injected, and the IF signal is extracted through an RF-blocking network, which does not couple to the TE_{10} mode.

Fig. 2 shows an experimental model of a mixer constructed in oversized microstrip. The monopole, diode-mounting lands, and RF-blocking network are all printed on a Mylar gasket whose thickness is 0.005 in. The conductor patterns were formed by photoetching copper and nichrome layers vacuum deposited on the Mylar, followed by a protective gold flash. The gasket is then sandwiched between two UG-385/U flanges, one of which is the input to a short-circuit termination. The other flange has been modified to accept a pair of rectangular choke grooves and a radial channel for the bias port. Each choke groove is a quarter wave deep and spaced a quarter wave from the main WR-15 waveguide. The choke was evaluated separately, by measuring the insertion loss through the main waveguide with an unmetallized 0.005-in Mylar gasket in place. The loss measured less than 0.2 dB across the 55–63-GHz band. A radial channel was next milled in the special flange to accommodate the bias line and RF-blocking network. This channel has a negligible effect on the insertion loss of the system.

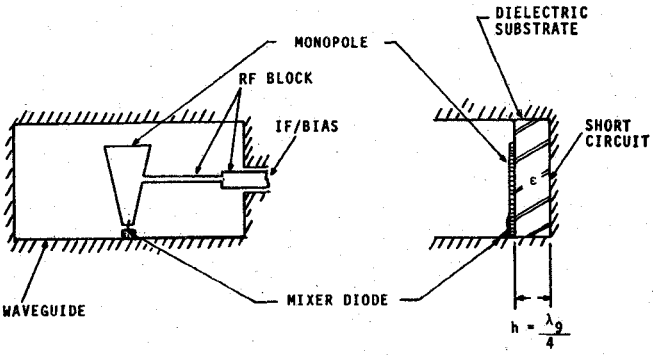

Fig. 1. Mixer in oversized microstrip.

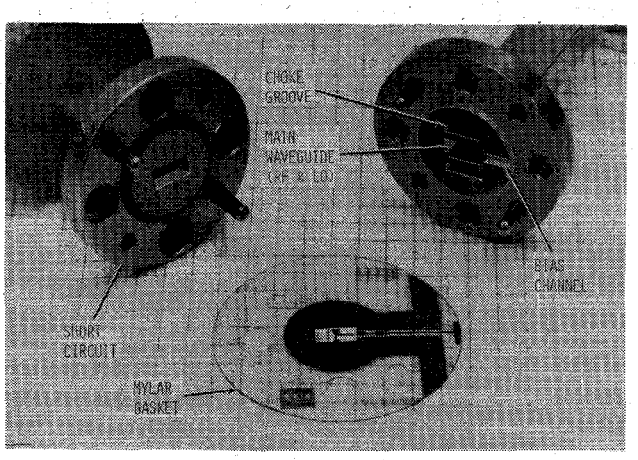

Fig. 2. Experimental mixer model.

The preliminary steps in the design of the oversized microstrip mixer included the selection of the optimum type of diode, and the impedance matching of the monopole to this diode. Optimum performance was obtained with preproduction samples of an advanced GaAs beam-lead Schottky-barrier diode. The diodes were developed by the British General Electric Company [3], and are expected to become commercially available in the near future.

Fig. 3 illustrates an advanced version of the oversized microstrip mixer, in which the monopole has been shortened and moved off axis to improve the impedance match. This mount also features a shielded miniature (SMA) output connector, which accommodates the high IF typically required in single-ended mixers. The Mylar was replaced by Kapton, as the latter can tolerate higher temperatures and, as such, is better suited to standard metallization and bonding techniques. With a forward bias of 0.6 V and 1.0 mW of drive, the VSWR of the final design was 2.0 or better across the band from 59 to 63 GHz. It is believed that further optimization of the shape and location of the monopole could result in still wider bandwidths. (Alternatively, enhanced performance across a narrow band, through suitable termination of the image frequency [4], is possible with a higher monopole Q.)

After a satisfactory impedance match had been obtained across a 4-GHz band, the noise figure of the mixer was measured. Measurements were performed by the standard Y-factor method with the aid of a noise tube calibrated against the AIL millimeter hot load [6]. An IF of 1.5 GHz was selected, as this frequency offers a good compromise between the degradation introduced by LO noise and

Manuscript received March 5, 1973; revised October 17, 1973. This work was supported by the Air Force Avionics Laboratory, WPAFB, under Contract F33615-C-1837.
The author is with the Applied Electronics Division, AIL, a division of Cutler–Hammer, Melville, N. Y. 11746.